Laser spectroscopy of metastable states in the $v=2$ cascade of antiprotonic ^{3}He

F. J. Hartmann, B. Ketzer, C. Maierl, R. Pohl,* and T. von Egidy
Physik-Department, Technische Universität München, D-85748 Garching, Germany

R. S. Hayano, M. Hori, T. Ishikawa, H. Tamura, and H. A. Torii
Department of Physics, University of Tokyo, 7-3-1 Hongo, Bunkyo-ku, Tokyo 113, Japan

M. Kumakura and N. Morita
Institute for Molecular Science, Myodaiji, Okazaki 444, Japan

I. Sugai
Institute for Nuclear Study, University of Tokyo, 3-2-1 Midori-cho, Tanashi, Tokyo 188, Japan

D. Horváth
Central Research Institute for Physics, Research Institute for Particle and Nuclear Physics, H-1525 Budapest, Hungary

J. Eades, E. Widmann,† and T. Yamazaki‡
CERN, CH-1211 Geneva 23, Switzerland

(Received 17 June 1998)

The pressure dependence of the metastable-state lifetimes in antiprotonic ^{3}He atoms $\bar{p}$-^{3}He$^+$ was studied using the recently observed laser resonance transition $(n,\ell)=(36,33)\rightarrow(35,32)$ in the $v=n-\ell-1=2$ cascade. To this end antiprotons from the Low Energy Antiproton Ring (LEAR) at CERN were extracted in approximately 200-ns-long bunches with about 10^8 $\bar{p}$ per bunch and stopped in a ^{3}He gas target. Time spectra of delayed annihilation products were taken with the help of a Čerenkov counter with a gated photomultiplier. Under our experimental conditions, $p=136-690$ mbars and $T=5.8$ K, the lowest metastable level (36,33) was found to be much shorter lived than the corresponding state (37,34) in the $v=2$ cascade of $\bar{p}$-^{4}He$^+$. It was strongly quenched at pressures above 500 mbars, whereas the higher states in the cascade remained nearly unaffected. This enabled us to investigate the $(37,34)\rightarrow(36,33)$ transition by resonant laser deexcitation. Its wavelength was found to be $\lambda=524.155\pm0.004$ nm, only 6 ppm lower than the theoretical value given by Korobov and Bakalov [Phys. Rev. Lett. **79**, 3379 1997)] after including relativistic corrections. [S1050-2947(98)06611-6]

PACS number(s): 36.10.Gv

I. INTRODUCTION

During the past five years metastable antiprotonic helium atoms have developed into an attractive laboratory for the exotic-atom formation and for the three-body interaction in the helium nucleus He^{2+} plus antiproton $\bar{p}$ plus electron $e^-\equiv\bar{p}$-^{3}He$^+$ system [1–9]. In particular, the observation of laser-induced transitions between metastable and short-lived states [5–9] has permitted the level scheme of metastable antiprotonic helium atoms to be studied with unprecedented accuracy. After a wealth of information had been collected for $\bar{p}$-^{4}He$^+$, some laser-stimulated transitions were also found in $\bar{p}$-^{3}He$^+$. The fact that the $\bar{p}$-^{3}He$^+$ data showed some unexpected peculiarities when compared with those from $\bar{p}$-^{4}He$^+$ [4,9] suggested that it would be very worthwhile to study the $\bar{p}$-^{3}He$^+$ atom in more detail.

*Present address: Eidgenössische Technische Hochschule, Zürich, Switzerland.

†Present address: Department of Physics, University of Tokyo, 7-3-1 Hongo, Bunkyo-ku, Tokyo 113, Japan.

‡Present address: Japan Society for the Promotion of Science, 5-3-1 Koji-machi, Chiyoda-ku, Tokyo 102, Japan.

II. THE METASTABLE $\bar{p}$-HELIUM ATOM

When antiprotons shot into helium are slowed down to kinetic energies lower than about the ionization potential of this element, they are captured by the Coulomb force to form $\bar{p}$-He$^+$ atoms [10,11], thereby ejecting one of the two electrons of the He atom. As has been shown by a number of experimental observations [5–9], states populated in the capture process have principal quantum numbers $n\approx\sqrt{M^*/m_e}$ (with M^* and m_e the reduced antiproton mass and the electron mass, respectively) that guarantee maximum overlap between the wave functions of the captured antiproton and of the ejected electron. This means, e.g., $n\approx38$ for $\bar{p}$-^{4}He$^+$ and $n\approx37$ for $\bar{p}$-^{3}He$^+$. Antiprotons captured into large-angular-momentum (ℓ) states form *metastable* $\bar{p}$-He$^+$ atoms with lifetimes of the order of microseconds [12] because the transitions to levels from which immediate annihilation is possible are suppressed.

Three facts contribute to this effect.

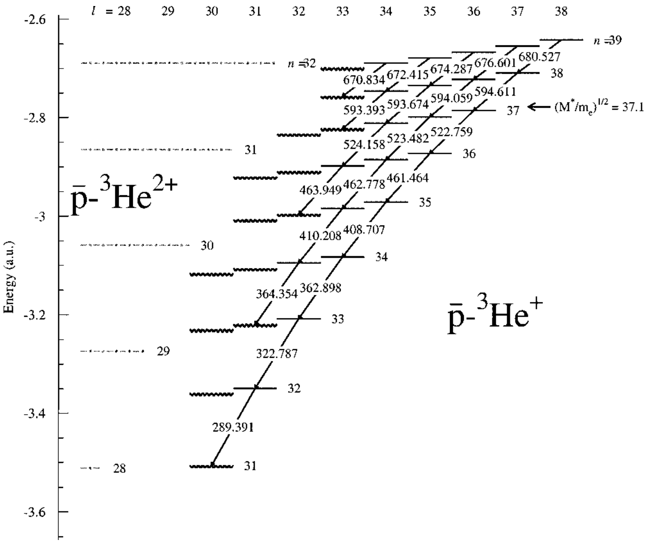

FIG. 1. Level scheme of the $\overline{p}$-^{3}He$^+$ atom and the $\overline{p}$-^{3}He^{2+} ion. The full lines denote metastable states, the wavy lines short-lived states in $\overline{p}$-^{3}He$^+$, and the dot-dashed lines states in $\overline{p}$-^{3}He^{2+}.

(i) Energy conservation requires that only Auger transitions with $\Delta n = n_{\text{final}} - n_{\text{initial}} \leqslant -4$ and consequently $\Delta \ell = \ell_{\text{final}} - \ell_{\text{initial}} \leqslant -4$ may occur. These are extremely slow [12].

(ii) Radiative transitions are also slow [13,14] due to the small transition energy ΔE available ($\Delta E \approx 2$ eV). The radiative rate for the decay of the (36,33) level in $\overline{p}$-^{3}He$^+$ was, e.g., calculated to be only about 0.8 μs^{-1} [13].

(iii) The Stark effect during collisions with other He atoms that usually induces sliding transitions with $\Delta n = 0$ is suppressed for two reasons: (a) the degeneracy of levels with the same n is removed by the influence of the remaining electron, thereby decreasing the transition probability appreciably [15], and (b) Pauli blocking between the remaining electron in $\overline{p}$-He$^+$ and the two electrons in the struck He atom prevents close encounters.

About 3% of all $\overline{p}$-He$^+$ atoms formed are metastable. This may be explained in terms of the initial ℓ distribution of the antiprotons in the exotic helium atom. It was pointed out some time ago [16] that, due to the flat kinetic-energy distribution of the exotic particle before capture and the range of possible impact parameters, the initial angular-momentum (ℓ) distribution has a downward-bent shape with a maximum at roughly half the maximum possible ℓ. Summing over the population of all metastable states $\ell \geqslant \ell_0 = 31$, the ℓ value at the border of the metastable regime (cf. Fig. 1) gives a total population of about 4% [14]. Considering the crudeness of this estimate, the result accounts astonishingly well for the observed trapping fraction of 3% [1,2].

The captured antiproton cascades down the ladder of metastable states (cf. Fig. 1) towards the shorter-lived levels (decay rate around 100 μs^{-1}) according to the propensity rule $\Delta n = \Delta \ell = -1$ predominantly along levels with $v = n - \ell - 1 = \text{const}$ [13,14]. All transitions with $\Delta n \neq -1$ are much slower due to the small overlap of the initial-state and final-state wave functions.

After formation, the $\overline{p}$-He$^+$ atom loses the kinetic energy (in the eV region) it has gained during the capture process by elastic collisions with other He atoms in the gas. In the hard-sphere approximation, the mean energy after k collisions is a constant fraction

$$f = \left[\frac{1-(1-\epsilon)^2}{2\epsilon} \right]^k$$

of the initial energy [17]. With m and M the ^{3}He and $\overline{p}$-^{3}He$^+$ masses, respectively, $\epsilon = 4mM/(m+M)^2 = 0.980$ and $f = 0.510^k$. Hence, after only $k \approx 10$ collisions the $\overline{p}$-He$^+$ atom is thermalized. As a rough guess we may take for the interaction potential the one governing the interaction between the kaonic atom $K^- e^-$-He^{2+} at principal quantum numbers around $n = 28$ and the He atom [18]. This gives roughly the same radius for the orbit of the exotic particle as in the $\overline{p}$ case. The radius at which this potential reaches 1 eV (repulsive) is about 10^{-8} cm, which leads to an elastic cross section of 3×10^{-16} cm^2 for exotic atoms with kinetic energies in the eV region. A thermalization time of well below 1 ns follows in He gas at 5.8 K and 500 mbar.

The overall lifetime of a metastable $\overline{p}$-He$^+$ atom in pure helium gas is limited by the number of metastable states the antiproton cascades through and by the mean lifetime of each state; in addition, quenching by collisions with other He atoms at impact parameters small enough to enable Stark mixing with short-lived states [19] will reduce the lifetime below this limit. Taking these effects together and assuming only binary collisions, the effective rate for annihilation may be written as

$$\lambda = \lambda_0 + \rho_{\text{atom}} \sigma_{\text{Stark}} \langle v \rangle, \tag{1}$$

with ρ_{atom} the He atomic density, σ_{Stark} the cross section for Stark mixing, and $\langle v \rangle$ the mean velocity of $\overline{p}$-He$^+$ relative to the helium atoms in the gas. In the time range of our observations (≈ 100 ns to ≈ 50 μs) the exotic atom is thermalized (see above), which results in a mean velocity

$$\langle v \rangle = \sqrt{\frac{8k_B T}{\pi M_{\text{red}}}} \approx 2.7 \times 10^4 \text{ cm/s at } 5.8 \text{ K},$$

with k_B the Boltzmann constant, T the temperature, and M_{red} the reduced mass of the $\overline{p}$-^{3}He$^+$ $-$ ^{3}He system.

There are two ways to gain insight into the nature of the metastable states in antiprotonic helium: (i) The gross information from the time between atomic capture and annihilation that determines the form of the delayed annihilation time spectrum (DATS) gives only information on the overall population and mean lifetime of all metastable states and (ii) laser-induced depopulation of individual metastable states towards short-lived levels provides information on the population and lifetime of the depopulated state, although only for a restricted number of levels.

Very soon during our experiments it became clear that isotope effects play a role in the $\overline{p}$-He$^+$ cascade. Thus it was found that the mean lifetime of the $\overline{p}$ was different in ^{3}He and in ^{4}He [2]. This difference may be attributed in part to effects in both capture and cascade that depend on the reduced mass M^* of the antiproton. Two of these are [14] that (i) the level spacing is inversely proportional to the square

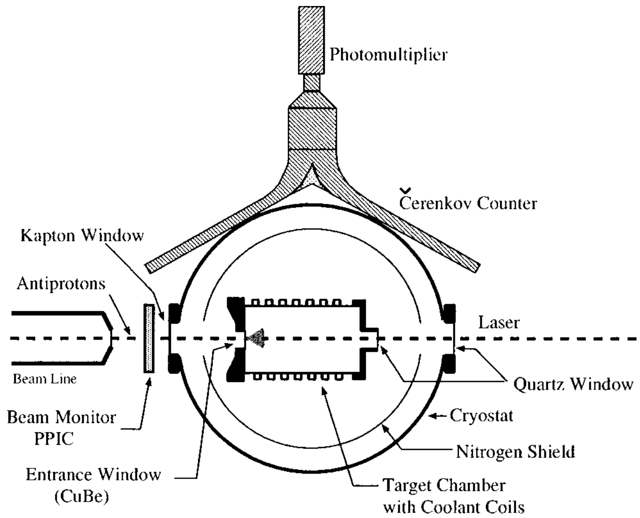

FIG. 2. Experimental arrangement for the fast-extraction studies. PPIC, the parallel plate ionization chamber.

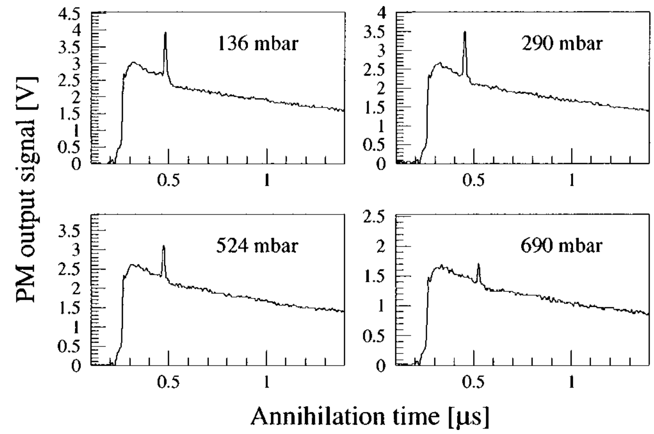

FIG. 3. Analog delayed annihilation time spectra for $\bar{p}$-^{3}He$^+$ at different pressures. The resonant deexcitation of the last metastable level manifests itself in the annihilation spikes seen. Their height decreases with increasing pressure due to the decreasing lifetime of the lowest level.

root of the reduced mass M^*, $\Delta E \approx M^* c^2 (\alpha Z)^2/n^3 \propto (M^*)^{-1/2}$, and (ii) the rate λ for radiative transitions depends on ΔE to the third power, $\lambda \propto (\Delta E)^3 \propto (M^*)^{-3/2}$. The total cascade time $\tau \propto [\Delta E \lambda]^{-1}$ hence is proportional to $(M^*)^2$. One expects a $\bar{p}$-He$^+$ lifetime that is larger in $\bar{p}$-^{4}He$^+$ by a factor

$$\left[\frac{M^*(\bar{p}-{}^4\mathrm{He}^{2+})}{M^*(\bar{p}-{}^3\mathrm{He}^{2+})}\right]^2 = 1.14,$$

a value very close to the one found from experiment, 1.144 ± 0.009 [4]. A closer look reveals further differences between $\bar{p}$-^{3}He$^+$ and $\bar{p}$-^{4}He$^+$: (i) The fraction of trapped antiprotons is lower by 22.2(4)% in $\bar{p}$-^{3}He$^+$ than in $\bar{p}$-^{4}He$^+$ at 5.8 K and pressures between 400 and 580 mbar [4] and (ii) a short-lived component in $\bar{p}$-^{3}He$^+$ (lifetime $\tau = 154 \pm 7$ ns) exists at 5.8 K and 400 mbar, which is not visible in $\bar{p}$-^{4}He$^+$ [4]. The reason for all this was not clear and it seemed to be necessary to study the $\bar{p}$-^{3}He$^+$ cascade in more detail. Very recently it has been revealed that the lifetime of the last metastable state in the $v=2$ cascade of $\bar{p}$-^{4}He$^+$, (37,34), shows a much stronger density dependence than the levels with larger n [20]. It is interesting to investigate this density dependence for the corresponding state in $\bar{p}$-^{3}He$^+$, (36,33), which may be depopulated by laser irradiation with a wavelength of 463.947 ± 0.002 nm [9]. If the lifetime of this state can be shortened by increasing the density, the upper transition $(37,34) \rightarrow (36,33)$ may also be investigated by laser resonance.

III. EXPERIMENTAL METHOD

Experimental setup

The experimental setup is shown in Fig. 2. Antiprotons of 200 MeV/c momentum were extracted from the Low Energy Antiproton Ring (LEAR) at CERN in bunches of about 200 ns length containing around 10^8 $\bar{p}$ per bunch (*fast extraction*). They were stopped in a target cooled down to 5.8 K and filled with ^{3}He gas (purity 99.998%) at pressures between 136 and 690 mbar. The (charged) pions from $\bar{p}$ annihilation were detected collectively (*analog method* [21]) with the help of a lucite Čerenkov counter of ≈ 2400 cm^2 area and 2 cm thickness, which was positioned close to the helium target and covered a solid angle for the annihilation pions of about 36% of 4π. The emitted Čerenkov light was fed into a photomultiplier via a light guide. One serious problem, however, existed: As 97% of the annihilations are prompt, the photomultiplier (PM) would be totally overloaded during the prompt annihilation period if one wanted to see the delayed annihilations with sufficient intensity. To remove this overloading, a gatable PM was developed by Hamamatsu Photonics Ltd. that could be switched on and off, respectively, within a few tens of nanoseconds. It had an on/off ratio of sensitivity of better than 1000:1 and very good integral linearity over the whole output-voltage operating range ($U \leq 20$ V into 50 Ω). The analog signal from this PM was recorded with a digital oscilloscope (Hewlett-Packard 54542A, with a bandwidth of 500 MHz, four channels at 2 G samples/s for each channel, and a resolution of eight bits). Finally the information was transferred from the digital oscilloscope to a computer and stored on disk and tape.

Four examples for an *analog delayed annihilation time spectrum* (ADATS) of this kind are shown in Fig. 3. Transitions from metastable to Auger-depopulated states were resonantly induced by a light pulse from an excimer-laser driven dye laser (≈ 4 mJ/pulse) shot into the target through a quartz window downstream along the beam. A detailed description of the laser system may be found in Ref. [22].

The *fast extraction* method has some advantages compared to the *slow extraction* method used in previous experiments.

(i) The laser is used much more efficiently as there are about 3×10^6 metastable $\bar{p}$-He$^+$ atoms in the target when the laser fires and not just one as in slow extraction [22]; consequently, only one laser shot is necessary to accumulate a whole ADATS.

(ii) Antiproton bunch and laser timing may be synchronized in such a way that the laser may be fired at any time

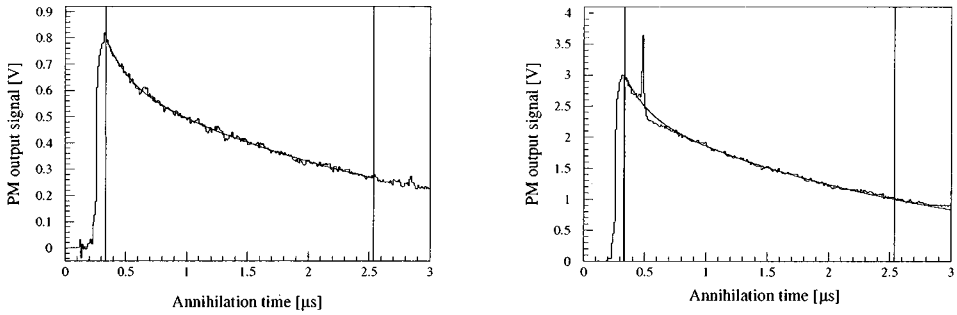

FIG. 4. (a) Fit to the *off-resonance* fast-extraction spectra. The double-exponential perfectly represents the data. (b) Typical depletion spectrum with the background from (a) overlaid. The vertical lines denote the borders of the fit region.

with respect to the antiproton bunch. With the conventional method [22] the laser could be triggered only after it became clear that *no* prompt annihilation had occurred. With a resulting minimum delay between prompt peak and laser ignition time of about 1.3 μs, only rather late times could be investigated.

IV. EXPERIMENTAL RESULTS

In the ADATS of Fig. 3 the laser-induced annihilation peak at about 500 ns is displayed for various gas pressures at a constant temperature $T=5.8$ K. Two methods are available to derive level lifetimes and populations.

One is variation of the delay time t of the laser shot (t scan). The metastable level can be emptied at variable time t by a sufficiently powerful laser pulse. From the intensity of the annihilation peak the population of the state may be derived as a function of the laser timing and an overall lifetime $T_v = 1/\lambda_v$ of the antiprotons in the cascade $v=$const may be extracted. It should be emphasized that T_v is *not* the lifetime of the last metastable state.

The other is the depletion-recovery method. The metastable level is emptied at time t by laser irradiation. It is refilled from higher states afterwards. The annihilation-time spectrum after the laser shot approaches the time spectrum without laser shot with the lifetime of the emptied metastable state [20]. The reliability of this method in fast extraction was tested by comparing the values for the lifetime of the (37,34) state in $\bar{p}$-^{4}He$^+$ derived by the depletion-recovery method in fast and slow extraction [23]. Very good agreement was found between the fast-extraction value $\tau_{(37,34)} = 137 \pm 21$ ns at a density of 4.88 ± 0.13 mol/l and the slow-extraction value $\tau_{(37,34)} = 128 \pm 25$ ns at a density of 4.56 ± 0.12 mol/l.

A. Data reduction

In order to extract level populations and lifetimes in $\bar{p}$-^{3}He$^+$ from the experimental data, peaks and decay parameters of the depletion have to be evaluated. In this context it is especially important to assign uncertainties to the measured voltages in the sampled analog spectra. Whereas in the normal delayed annihilation time spectrum (DATS) the error in intensity in each channel is given by the square root of the number of annihilations seen in the corresponding time bin Δt, in the ADATS the number of charged particles hitting the Čerenkov radiator and the number of photoelectrons emitted from the photocathode of the PM for each charged particle determine the error for each time bin [24]. Furthermore, digitizing errors in the oscilloscope exist, which, however, may be minimized by carefully adjusting the oscilloscope sensitivity.

Unfortunately, it is rather difficult to get a reliable value for the number N_{ph} of photons reaching the photocathode, as the light collection in Čerenkov counter and light guide is hard to evaluate; also the attempt to determine N_{ph} from the anode-signal peak height, the gain of the PM, and the quantum efficiency of its photocathode suffers from uncertainties. Therefore, a statistical test was used to derive the error of the voltage measured in each bin from the voltage fluctuations. To this end a small region of the ADATS was fitted, which (i) could be perfectly described by an exponential and where (ii) digitizing errors played no role. With bin errors equal to $\sqrt{V}$ the values of $\sqrt{\chi^2_\nu}$, the square root of the reduced χ^2, was evaluated. $\sqrt{\chi^2_\nu}$ is just the factor each bin error has to be multiplied by to attain the correct voltage-height error. Digitizing errors were added afterwards in quadrature.

Another problem in the evaluation of the depletion-recovery spectra concerned the fit of the ADATS without laser shot. Fortunately, only the area of the laser peak (in the case of the t-scan method) or the slope in the trailing edge of the negative depletion peak (in the case of the depletion-recovery method) had to be evaluated. Nevertheless, a reliable fitting procedure was mandatory.

The off-resonance ADATS in the analog method stems from two sources: (i) the pions from delayed $\bar{p}$ annihilation, which fade away with the overall lifetime of the metastable states and lead to a short-lived component with a lifetime τ of several hundred nanoseconds and a longer-lived one with $\tau \approx 3$ μs in the DATS [4], and (ii) the positrons from the decay of μ^+ (lifetime 2.2 μs) generated by the decay of prompt-annihilation π^+ stopped in the experimental environment. By fitting the ADATS with very late laser pulses by the sum of two exponentials,

$$I(t) = A \exp(-\lambda_{\text{short}} t) + B \exp(-\lambda_{\text{long}} t),$$

reliable off-resonance time spectra could be derived. A typical fit result is shown in Fig. 4.

B. Density dependence of the t-scan decay rate

The time development of the (36,33)-level population was determined with the t-scan method described above.

TABLE I. Decay rates $\lambda_{v=2}$ ($n>36$) and $\lambda_{(36,33)}$ as functions of the ^{3}He density.

Density (mol/l)	Density (10^{20} cm^{-3})	$\lambda_{v=2}$ ($n>36$) (μs^{-1})	$\lambda_{(36,33)}$ (μs^{-1})
0.29±0.05	1.8±0.3	0.80±0.12	8.6±1.1
0.62±0.06	3.7±0.3	0.93±0.16	9.2±0.9
1.13±0.06	6.8±0.4	1.16±0.24	10.8±1.5
1.52±0.06	9.1±0.4	1.05±0.38	16.3±2.4

Nine shots from one LEAR spill were used for each of the four target pressures investigated.

The results for $\lambda_{v=2}$ ($n>36$) are shown in Table I, third column. Figure 5(a) depicts them as a function of density (full squares). Also shown in this figure (as a full line) is the result for $\lambda_{v=2}$ as derived from the fit of a straight line to the decay-rate data [cf. Eq. (1)].

C. Density dependence of the (36,33) lifetime

The decay rate $\lambda_{(36,33)}$ of the (36,33) level was directly determined by the depletion-recovery method. The results are given in Table I, fourth column. This rate is shown in Fig. 5(b) (full circles). The result of a linear fit to these λ values [cf. Eq. (1)] is depicted as a dashed line in the figure. Astonishing enough, the decay rate in the limit of zero density,

$$\lambda_{(36,33)}(\rho_{\text{atom}}=0)=6.7\pm1.3\,\mu\text{s}^{-1},$$

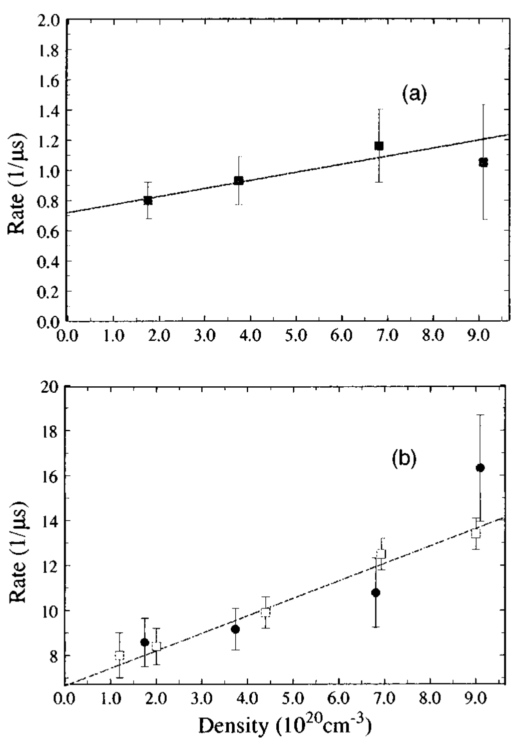

FIG. 5. Rates in the $v=2$ cascades of $\bar{p}$-^{3}He$^+$ and $\bar{p}$-^{4}He$^+$. (a) Data for $\lambda_{v=2}$ in $\bar{p}$-^{3}He$^+$ (full squares). The full line denotes the linear fit to the data. (b) Data for $\lambda_{(36,33)}$. Full circles, experimental $\bar{p}$-^{3}He$^+$ data; dashed line, fit to the experimental data; open squares, experimental data for $\lambda_{(37,34)}$ in $\bar{p}$-^{4}He, multiplied by a factor of 10.

TABLE II. Comparison of quenching cross sections in $\bar{p}$-^{3}He$^+$ and $\bar{p}$-^{4}He$^+$.

Level	$\sigma_{\text{Stark}}(10^{-19}$ cm$^2)$
$\bar{p}$-^{3}He$^+$(36,33)	$3.0^{+0.9}_{-1.0}$
$\bar{p}$-^{4}He$^+$(37,34)	0.52±0.03

is about a factor of 4 larger than the sum of the calculated radiation and Auger rates, $\lambda=1.7\,\mu$s^{-1} [25,26]. Assuming a quadratic density dependence, as it might be expected when three-body collisions play a role, makes the agreement even worse.

From the same fit we obtained

$$[\sigma_{\text{Stark}}]_{(36,33)}\langle v\rangle=8.0^{+2.3}_{-2.7}\times10^{-15}\,\text{cm}^3\ \text{s}^{-1}.$$

Since in the time range of the fit the $\bar{p}$-^{3}He$^+$ atoms are totally thermalized, $\langle v\rangle=2.7\times10^4$ cm s^{-1}, a cross section

$$\sigma_{\text{Stark}}=3.0^{+0.9}_{-1.0}\times10^{-19}\,\text{cm}^2$$

follows. This cross section is much smaller than the geometrical cross section. Apparently only a small fraction of the collisions with He atoms lead to Stark mixing with subsequent fast Auger deexcitation and annihilation.

A comparison of the (36,33) decay rate with that of the (37,34) level in $\bar{p}$-^{4}He$^+$ [20], shown, multiplied by ten, as open squares in Fig. 5(b), reveals that the intrinsic decay rate of the last metastable state is about a factor of 10 smaller in $\bar{p}$-^{4}He$^+$ than in $\bar{p}$-^{3}He$^+$ and quenching is much less efficient in the case of $\bar{p}$-^{4}He$^+$. The reason for this phenomenon is not yet clear. Table II gives a comparison of the corresponding quenching cross sections.

The large difference at low density between the $v=2$ cascade lifetime $T_{v=2}=1/\lambda_{v=2}$ and $\tau_{(36,33)}=1/\lambda_{(36,33)}$ indicates that there are other metastable states above the (36,33) level in this cascade. However, not all of them are quenched as efficiently as the lowest one: $\lambda_{v=2}$ increases with density only to $\lambda_{v=2}\approx1\,\mu$s^{-1} at 1.5 mol/l [cf. Table I]. Evidently, the metastable states above the lowest one retain their longevity. This opened up the very interesting possibility to directly observe transitions $(37,34)\rightarrow(36,33)$ resonantly induced by laser irradiation, as in the case of $\bar{p}$-^{4}He$^+$ [20]: The still long-lived upper state (37,34) is emptied by laser irradiation to the lower state, which has been made short-lived by density quenching, and a $\bar{p}$ annihilation peak may be observed. The shape of this annihilation peak gives direct information on the (36,33)-level lifetime.

D. Resonance scan on the transition $(37,34)\rightarrow(36,33)$

For the resonance scan, performed at 690 mbar pressure, the peak intensity of the resonance spike was determined as a function of wavelength, with the background subtraction similar to that for the depletion analysis. The scan was considerably facilitated by the apparently reliable predictions for the transition energies in $\bar{p}$-He$^+$ [27,28]. Figure 6 shows a typical resonance spike with its slow decay and Fig. 7 depicts the result of the scan together with a fit by a Gaussian

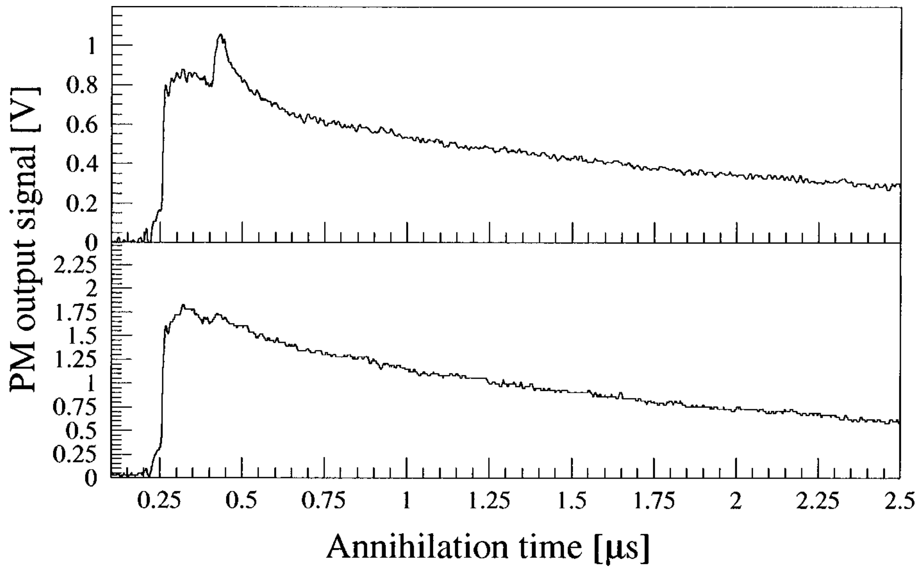

FIG. 6. (a) Resonance spike in the ADATS generated by the laser-induced transition (37,34)→(36,33) in $\bar{p}$-^{3}He$^+$, taken at $\lambda = 524.155$ nm. (b) Off-resonance data, taken at a wavelength smaller by 26 pm.

with fixed width ($\Gamma_{\rm Gauss} = 7$ pm, to account for the finite bandwidth of the laser) convoluted with a Lorentzian (width free). From this fit an experimental value

$$\lambda_{\rm expt}[(37,34)\rightarrow(36,33)] = 524.155 \pm 0.004 \text{ nm}$$

for the resonance wavelength was found at $\rho_{\rm atom} = 9.1 \times 10^{20}$ cm^{-3}. The error includes a 3-pm uncertainty of the wavelength calibration. The λ value differs by less than 6 ppm from the theoretical prediction for an isolated atom, $\lambda_{\rm th} = 524.158$ nm [28], which includes the corrections for the relativistic motion of the e^-. A small positive difference $\Delta\lambda = \lambda_{\rm th} - \lambda_{\rm expt}$, observed here at low statistical significance, was already seen for other transitions; it may be attributed to missing additional corrections in the calculation.

The decay of the laser-induced annihilation peak could be adequately fitted by an exponential. The resulting lifetime $\tau_{(36,33)} = 42.2 \pm 2.6$ ns is in reasonable agreement with the result derived from the depletion spectrum at 690 mbar, $\tau_{(36,33)} = 52.6 \pm 7.7$ ns.

V. SUMMARY AND CONCLUSIONS

The $v = 2$ cascade in antiprotonic ^{3}He has been investigated. The last metastable level in this cascade ($n = 36, \ell = 33$) has an intrinsic decay rate of 6.7 ± 1.3 μs^{-1}, which is by a factor of 8 larger than the radiative rate and about three times larger than the value calculated for the sum of Auger and radiative rates. It is quenched with a cross section of $\sigma_{\rm Stark} = 3.0^{+0.9}_{-1.0} \times 10^{-19}$ cm^2. At higher pressure values only the lowest metastable level (36,33) is quenched, this, however, to an extent that enabled the feeding transition (37,34)→(36,33) to be investigated by laser-resonance spectroscopy. The wavelength of this transition was found to be $\lambda_{\rm expt}[(37,34)\rightarrow(36,33)] = 524.155 \pm 0.004$ nm, only

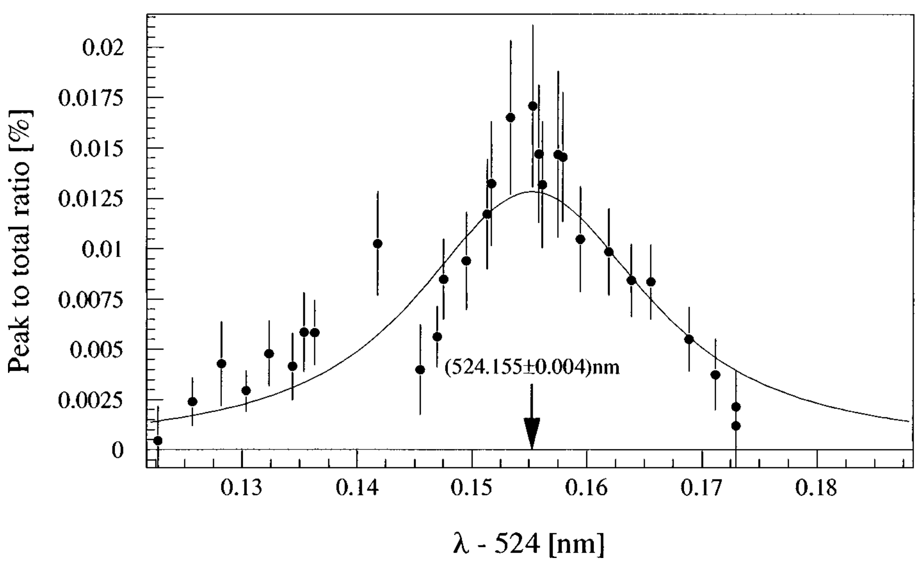

FIG. 7. Resonance curve for the 524-nm transition (37,34)→(36,33) in $\bar{p}$-^{3}He$^+$.

6 ppm smaller than the theoretical prediction of Korobov, which includes the relativistic corrections.

ACKNOWLEDGMENTS

We would like to cordially thank the LEAR and PS staffs for providing us with the high-intensity fast-extraction $\overline{p}$ beam. The present work is supported by the German Bundesministerium für Bildung, Wissenschaft, Forschung und Technologie, a Grant-in-Aid for Specially Promoted Research and for International Scientific Research of the Japanese Ministry of Education, Science and Culture, the Japanese Society for the Promotion of Science (JSPS), and the Hungarian National Science Foundation.

[1] M. Iwasaki, S. N. Nakamura, K. Shigaki, Y. Shimizu, H. Tamura, T. Ishikawa, R. S. Hayano, E. Takada, E. Widmann, H. Outa, M. Aoki, P. Kitching, and T. Yamazaki, Phys. Rev. Lett. **67**, 1246 (1991).

[2] T. Yamazaki, E. Widmann, R. S. Hayano, M. Iwasaki, S. N. Nakamura, K. Shigaki, F. J. Hartmann, H. Daniel, T. von Egidy, P. Hofmann, Y.-S. Kim, and J. Eades, Nature (London) **361**, 238 (1993).

[3] S. N. Nakamura, R. S. Hayano, M. Iwasaki, K. Shigaki, E. Widmann, T. Yamazaki, H. Daniel, T. von Egidy, F. J. Hartmann, P. Hofmann, Y.-S. Kim, and J. Eades, Phys. Rev. A **49**, 4457 (1994).

[4] B. Ketzer, F. J. Hartmann, H. Daniel, T. von Egidy, W. Müller, W. Schmid, E. Widmann, I. Sugai, H. Masuda, T. Yamazaki, R. S. Hayano, F. E. Maas, H. A. Torii, N. Morita, M. Kumakura, D. Horváth, and J. Eades, Phys. Rev. A **53**, 2108 (1996).

[5] N. Morita, M. Kumakura, T. Yamazaki, E. Widmann, H. Masuda, I. Sugai, R. S. Hayano, F. E. Maas, H. A. Torii, F. J. Hartmann, H. Daniel, T. von Egidy, B. Ketzer, W. Müller, W. Schmid, D. Horváth, and J. Eades, Phys. Rev. Lett. **72**, 1180 (1994).

[6] R. S. Hayano, F. E. Maas, H. A. Torii, N. Morita, M. Kumakura, T. Yamazaki, H. Masuda, I. Sugli, F. J. Hartmann, H. Daniel, T. von Egidy, B. Ketzer, W. Müller, W. Schmid, D. Horváth, J. Eades, and E. Widmann, Phys. Rev. Lett. **73**, 1485 (1994); **73**, 3181(E) (1994).

[7] F. E. Maas, R. S. Hayano, T. Ishikawa, H. Tamura, H. A. Torii, N. Morita, T. Yamazaki, I. Sugai, K. Nakayoshi, F. J. Hartmann, H. Daniel, T. von Egidy, B. Ketzer, A. Niestroj, S. Schmid, W. Schmid, D. Horváth, J. Eades, and E. Widmann, Phys. Rev. A **52**, 4266 (1995).

[8] B. Ketzer, F. J. Hartmann, T. von Egidy, C. Maierl, R. Pohl, J. Eades, E. Widmann, T. Yamazaki, M. Kumakura, N. Morita, R. S. Hayano, M. Hori, T. Ishikawa, H. A. Torii, I. Sugai, and D. Horváth, Phys. Rev. Lett. **78**, 1671 (1997).

[9] H. A. Torii, M. Hori, T. Ishikawa, F. E. Mass, R. S. Hayano, N. Morita, M. Kumakura, I. Sugai, B. Ketzer, H. Daniel, F. J. Hartmann, R. Pohl, R. Schmidt, T. von Egidy, D. Horváth, J. Eades, E. Widmann, and T. Yamazaki, Phys. Rev. A **53**, R1931 (1996).

[10] W. A. Beck, L. Wilets, and M. A. Alberg, Phys. Rev. A **48**, 2779 (1993).

[11] G. Ya. Korenman, Hyperfine Interact. **101/102**, 81 (1996).

[12] J. E. Russell, Phys. Rev. A **1**, 721 (1970); **1**, 735 (1970); **1**, 742 (1970).

[13] I. Shimamura, Phys. Rev. A **46**, 3776 (1992).

[14] T. Yamazaki and K. Ohtsuki, Phys. Rev. A **45**, 7782 (1992).

[15] W. E. Lamb and R. C. Retherford, Phys. Rev. **79**, 549 (1950).

[16] H. Daniel, Z. Phys. A **302**, 195 (1981).

[17] E. U. Condon and G. Breit, Phys. Rev. **49**, 229 (1936).

[18] J. E. Russell, Phys. Rev. **188**, 187 (1969).

[19] G. Ya. Korenman, M.V. Lomonosov Moscow State University, D.V. Skobeltsyn Institute of Nuclear Physics Report No. MSU 97-I/452, 1997 (unpublished).

[20] M. Hori, H. A. Torii, R. S. Hayano, T. Ishikawa, F. E. Maas, H. Tamura, B. Ketzer, F. J. Hartmann, R. Pohl, C. Maierl, M. Hasinoff, T. von Egidy, M. Kumakura, N. Morita, I. Sugai, D. Horváth, E. Widmann, J. Eades, and T. Yamazaki, Phys. Rev. A **58**, 1612(E) (1998).

[21] A. Niestroj, F. J. Hartmann, H. Daniel, B. Ketzer, T. von Egidy, F. E. Mass, R. S. Hayano, T. Ishikawa, H. Tamura, H. A. Torii, N. Morita, T. Yamazaki, I. Sugai, K. Nakayoshi, D. Horváth, J. Eades, and E. Widmann, Nucl. Instrum. Methods Phys. Res. A **373**, 411 (1996).

[22] H. A. Torii, R. S. Hayano, F. E. Mass, N. Morita, M. Kumakura, T. Yamazaki, H. Masuda, I. Sugai, B. Ketzer, F. J. Hartmann, H. Daniel, T. von Egidy, W. Müller, W. Schmid, and D. Horváth, Nucl. Instrum. Methods Phys. Res. A **396**, 257 (1997).

[23] C. Maierl, Diploma thesis, Technische Universität München, 1997 (unpublished).

[24] Y. Kawashima, Y. Watanabe, and T. Yamazaki, Nucl. Instrum. Methods Phys. Res. A **274**, 241 (1989).

[25] P. T. Greenland and R. Thürwächter, Hyperfine Interact. **76**, 355 (1993).

[26] V. I. Korobov and I. Shimamura, Phys. Rev. A **56**, 4587 (1997).

[27] V. I. Korobov, Phys. Rev. A **54**, R1749 (1996).

[28] V. I. Korobov and D. D. Bakalov, Phys. Rev. Lett. **79**, 3379 (1997).